# Supporting information: A Genetic Algorithm for Universal Optimization of Ultrasensitive Surface Plasmon Resonance Sensors with 2D Materials

Matej Sebek,[*,†,‡] Thanh Thi Kim Nguyen,[†] Xiaodi Su,[‡] and Jinghua Teng[*,‡]

†*UCL Healthcare Biomagnetic and Nanomaterials Laboratories, 21 Albemarle Street, London W1S 4BS Biophysics Group, London WC1E 6BT, United Kingdom*

‡*Institute of Materials Research and Engineering, Agency for Science, Technology and Research, Innovis, Singapore, 138634 Singapore*

E-mail: matej.sebek.17@ucl.ac.uk; jh-teng@imre.a-star.edu.sg

Table 1: Table of dielectric constants of materials in the database at $\lambda = 633$ and $\lambda = 875$ nm and a minimum thickness step used

| **Material** | $\epsilon_r$ **at 633 nm** | $\epsilon_i$ **at 633 nm** | $\epsilon_r$ **at 785 nm** | $\epsilon_i$ **at 785 nm** | **Thickness step [nm]** |
|---|---|---|---|---|---|
| Ag | -18.311 | 0.481 | -29.817 | 0.377 | 1.000 |
| $Ag_3AsS_3$ | 9.009 | 0.000 | 8.384 | 0.000 | 1.000 |
| AgBr | 5.027 | 0.000 | NaN | NaN | 1.000 |
| AgCl | 4.231 | 0.000 | 4.147 | 0.000 | 1.000 |
| $AgGaS_2$ | 6.494 | 0.000 | 6.220 | 0.000 | 1.000 |
| $AgGaSe_2$ | 7.818 | 0.000 | NaN | NaN | 1.000 |
| Al | -34.212 | 0.909 | -53.170 | 1.734 | 1.000 |
| $Al_2O_3$ | 2.813 | 0.000 | 2.794 | 0.000 | 1.000 |
| AlAs | 9.671 | 0.000 | 9.064 | 0.000 | 1.000 |
| AlSb | 14.974 | 1.140 | 12.733 | 0.639 | 1.000 |
| $As_2S_3$ | 6.380 | 0.000 | NaN | NaN | 0.480 |
| Au | -11.771 | 1.258 | -22.882 | 1.426 | 1.000 |
| $B_4C$ | 10.304 | 3.157 | 10.526 | 2.366 | 1.000 |
| $BaB_2O_4$ | 2.779 | 0.000 | 2.758 | 0.000 | 1.000 |
| $BaF_2$ | 2.170 | 0.000 | 2.163 | 0.000 | 1.000 |
| $BaTiO_3$ | 5.781 | 0.000 | NaN | NaN | 1.000 |
| Be | 1.671 | 21.839 | 0.415 | 22.944 | 1.000 |
| BeO | 2.948 | 0.000 | 2.934 | 0.000 | 1.000 |
| Bi | -4.711 | 14.388 | -6.432 | 20.428 | 1.000 |
| $Bi_4Ge_3O1_2$ | 4.398 | 0.000 | 4.297 | 0.000 | 1.000 |
| $Bi_4Ti_3O1_2$ | 7.538 | 0.000 | NaN | NaN | 1.000 |
| $Bi1_2GeO_20$ | 6.470 | 0.000 | NaN | NaN | 1.000 |
| $Bi1_2SiO_20$ | 6.391 | 0.000 | NaN | NaN | 1.000 |
| $BiB_3O6$ | 3.795 | 0.000 | 3.743 | 0.000 | 1.000 |
| $BiFeO_3$ | 8.807 | 0.000 | 8.088 | 0.000 | 1.000 |
| h-BN | 4.856 | 0.000 | 4.762 | 0.000 | 0.350 |
| a-BP | 6.803 | 2.834 | 8.349 | 2.435 | 0.530 |
| b-BP | 6.972 | 0.243 | 9.027 | 0.081 | 0.530 |
| C | 5.616 | 7.399 | 5.821 | 8.762 | 0.350 |
| Ca | -7.924 | 1.679 | -13.187 | 2.553 | 1.000 |
| $CaCO_3$ | 2.741 | 0.000 | 2.720 | 0.000 | 1.000 |
| $CaF_2$ | 2.053 | 0.000 | 2.047 | 0.000 | 1.000 |
| $CaMoO_4$ | 3.942 | 0.000 | 3.881 | 0.000 | 1.000 |
| $CaWO_4$ | 3.667 | 0.000 | 3.622 | 0.000 | 1.000 |
| CdS | 5.682 | 0.000 | 5.344 | 0.000 | 1.000 |
| CdTe | 8.616 | 1.649 | 8.697 | 0.617 | 1.000 |
| $CeF_3$ | 2.648 | 0.010 | 2.635 | 0.008 | 1.000 |
| Co | -12.507 | 18.467 | -16.502 | 23.349 | 1.000 |
| Cr | -1.139 | 20.815 | -2.059 | 21.607 | 1.000 |
| Cs | -1.447 | 0.647 | -2.850 | 0.972 | 1.000 |

| Material | $\epsilon_r$ at 633 nm | $\epsilon_i$ at 633 nm | $\epsilon_r$ at 785 nm | $\epsilon_i$ at 785 nm | Thickness step [nm] |
|---|---|---|---|---|---|
| CsBr | 2.868 | 0.000 | 2.838 | 0.000 | 1.000 |
| CsCl | 2.681 | 0.000 | 2.660 | 0.000 | 1.000 |
| CsF | 2.181 | 0.000 | 2.173 | 0.000 | 1.000 |
| CsI | 3.172 | 0.000 | 3.123 | 0.000 | 1.000 |
| CsLiB6O10 | 2.237 | 0.000 | 2.227 | 0.000 | 1.000 |
| Cu | -28.274 | 7.139 | -49.172 | 14.609 | 1.000 |
| CuCl | 3.634 | 0.000 | 3.623 | 0.000 | 1.000 |
| $CuGaS_2$ | 7.139 | 0.000 | 6.740 | 0.000 | 1.000 |
| $Dy_2O_3$ | 3.881 | 0.000 | NaN | NaN | 1.000 |
| Fe | -50.946 | 24.727 | -90.730 | 70.118 | 1.000 |
| $Fe_2O_3$ | 9.761 | 0.441 | 8.219 | 0.109 | 1.000 |
| $Fe_3O_4$ | 5.550 | 0.694 | 5.224 | 0.575 | 1.000 |
| GaAs | 13.776 | 1.397 | 13.003 | 0.700 | 1.000 |
| GaN | 5.240 | 0.279 | 5.061 | 0.241 | 1.000 |
| GaP | 11.258 | 0.000 | 10.570 | 0.000 | 1.000 |
| GaS | 7.372 | 0.000 | 7.093 | 0.000 | 0.466 |
| GaSb | 24.082 | 12.535 | 17.807 | 3.203 | 1.000 |
| Ge | 10.706 | 2.713 | 9.908 | 0.645 | 1.000 |
| $GeO_2$ | 2.577 | 0.000 | 2.556 | 0.000 | 1.000 |
| Hg | -23.450 | 20.735 | -29.379 | 34.156 | 1.000 |
| HgS | 8.322 | 0.000 | 7.705 | 0.000 | 1.000 |
| In | -27.174 | 9.134 | -40.522 | 16.506 | 1.000 |
| InAs | 14.815 | 4.699 | 13.104 | 2.633 | 1.000 |
| InP | 11.024 | 2.032 | 11.471 | 1.794 | 1.000 |
| InSb | 19.019 | 18.461 | 20.393 | 6.874 | 1.000 |
| K | -3.016 | 0.179 | -5.336 | 0.198 | 1.000 |
| KBr | 2.423 | 0.000 | 2.401 | 0.000 | 1.000 |
| KCl | 2.214 | 0.000 | 2.200 | 0.000 | 1.000 |
| KF | 1.854 | 0.000 | 1.849 | 0.000 | 1.000 |
| $KH_2PO_4$ | 2.272 | 0.000 | 2.256 | 0.000 | 1.000 |
| KI | 2.758 | 0.000 | 2.719 | 0.000 | 1.000 |
| $KNbO_3$ | 5.438 | 0.000 | 5.262 | 0.000 | 1.000 |
| $KTaO_3$ | 4.959 | 0.000 | 4.822 | 0.000 | 1.000 |
| $KTiOPO_4$ | 3.477 | 0.000 | 3.407 | 0.000 | 1.000 |
| $LaF_3$ | 2.508 | 0.002 | 2.499 | 0.002 | 1.000 |
| Li | -9.400 | 0.923 | -15.454 | 1.381 | 1.000 |
| $LiB_3O_5$ | 2.618 | 0.000 | 2.606 | 0.000 | 1.000 |
| LiBr | 3.179 | 0.000 | 3.171 | 0.000 | 1.000 |
| LiCaAlF6 | 1.938 | 0.000 | 1.934 | 0.000 | 1.000 |
| LiCl | 2.760 | 0.000 | 2.755 | 0.000 | 1.000 |
| LiF | 1.936 | 0.000 | 1.930 | 0.000 | 1.000 |
| LiI | 3.819 | 0.000 | 3.812 | 0.000 | 1.000 |
| $LiIO_3$ | 3.537 | 0.000 | 3.487 | 0.000 | 1.000 |

| Material | $\epsilon_r$ at 633 nm | $\epsilon_i$ at 633 nm | $\epsilon_r$ at 785 nm | $\epsilon_i$ at 785 nm | Thickness step [nm] |
|---|---|---|---|---|---|
| $LiNbO_3$ | 5.228 | 0.000 | 5.095 | 0.000 | 1.000 |
| $Lu_2O_3$ | 3.726 | 0.000 | NaN | NaN | 1.000 |
| $LuAl_3(BO_3)_4$ | 3.160 | 0.000 | 3.143 | 0.000 | 1.000 |
| Mg | -34.419 | 4.799 | -55.951 | 10.650 | 1.000 |
| $MgAl_2O_4$ | 2.937 | 0.000 | 2.917 | 0.000 | 1.000 |
| $MgF_2$ | 2.020 | 0.002 | 2.015 | 0.001 | 1.000 |
| MgO | 3.013 | 0.000 | NaN | NaN | 1.000 |
| Mn | -6.437 | 18.123 | -8.104 | 21.872 | 1.000 |
| Mo | -76.628 | 14.588 | -124.214 | 35.263 | 1.000 |
| $MoO_3$ | 4.342 | 0.105 | 4.202 | 0.366 | 1.356 |
| $MoS_2$ | 16.263 | 9.287 | 12.279 | 0.000 | 0.650 |
| $MoSe_2$ | 26.242 | 9.623 | 29.685 | 6.789 | 0.650 |
| $MoTe_2$ | 12.871 | 12.316 | 19.522 | 12.285 | 0.700 |
| $NH_4H_2PO_4$ | 2.316 | 0.000 | 2.298 | 0.000 | 1.000 |
| Na | -6.918 | 0.265 | -11.430 | 0.343 | 1.000 |
| NaBr | 2.686 | 0.000 | 2.657 | 0.000 | 1.000 |
| NaCl | 2.376 | 0.000 | 2.359 | 0.000 | 1.000 |
| NaF | 1.754 | 0.000 | 1.750 | 0.000 | 1.000 |
| NaI | 3.129 | 0.000 | 3.085 | 0.000 | 1.000 |
| Nb | -5.606 | 14.926 | -9.850 | 15.442 | 1.000 |
| $Nb_2O_5$ | 5.389 | 0.000 | 5.214 | 0.000 | 1.000 |
| Ni | -39.027 | 16.575 | -70.076 | 38.290 | 1.000 |
| Os | 21.935 | 19.409 | 9.367 | 11.809 | 1.000 |
| Pb | -39.304 | 13.470 | -55.624 | 17.379 | 1.000 |
| $Pb_5Ge_3O11$ | 4.462 | 0.000 | NaN | NaN | 1.000 |
| $PbF_2$ | 3.101 | 0.000 | 3.061 | 0.000 | 1.000 |
| $PbMoO_4$ | 5.462 | 0.000 | 5.339 | 0.000 | 1.000 |
| PbSe | 19.934 | 18.771 | 23.110 | 18.435 | 1.000 |
| $PbTiO_3$ | 7.132 | 0.000 | 6.839 | 0.000 | 1.000 |
| Pd | -27.525 | 3.154 | -47.098 | 2.864 | 1.000 |
| Pt | -37.407 | 5.731 | -62.234 | 8.924 | 1.000 |
| Rb | -2.213 | 0.315 | -3.978 | 0.425 | 1.000 |
| RbBr | 2.403 | 0.000 | 2.381 | 0.000 | 1.000 |
| RbCl | 2.219 | 0.000 | 2.205 | 0.000 | 1.000 |
| RbF | 1.951 | 0.000 | 1.943 | 0.000 | 1.000 |
| RbI | 2.697 | 0.000 | 2.661 | 0.000 | 1.000 |
| $RbTiOPO_4$ | 3.598 | 0.000 | 3.527 | 0.000 | 1.000 |
| Rh | -4.565 | 20.832 | NaN | NaN | 1.000 |
| $Sc_2O_3$ | 3.362 | 0.000 | NaN | NaN | 1.000 |
| Se | 2.041 | 0.026 | 1.874 | 0.000 | 1.000 |
| $Si_3N_4$ | 4.159 | 0.000 | 4.101 | 0.000 | 1.000 |
| SiC | 11.417 | 1.855 | 11.023 | 1.113 | 1.000 |
| SiO | 0.000 | 0.000 | 0.000 | 0.000 | 1.000 |
| $SiO_2$ | 2.142 | 0.005 | 2.134 | 0.004 | 1.000 |
| Sn | -38.241 | 30.837 | NaN | NaN | 1.000 |

| **Material** | $\epsilon_r$ **at 633 nm** | $\epsilon_i$ **at 633 nm** | $\epsilon_r$ **at 785 nm** | $\epsilon_i$ **at 785 nm** | **Thickness step [nm]** |
|---|---|---|---|---|---|
| a-SnSe | 38.065 | 71.275 | NaN | NaN | 0.900 |
| d-SnSe | -59.945 | 159.989 | NaN | NaN | 0.900 |
| e-SnSe | 4.006 | 15.539 | NaN | NaN | 0.900 |
| $SrF_2$ | 2.065 | 0.000 | 2.059 | 0.000 | 1.000 |
| $SrMoO_4$ | 3.620 | 0.000 | 3.569 | 0.000 | 1.000 |
| $SrTiO_3$ | 5.701 | 0.000 | 5.499 | 0.000 | 1.000 |
| Ta | -31.151 | 12.012 | -50.148 | 14.245 | 1.000 |
| $Ta_2O_5$ | 4.386 | 0.030 | 4.299 | 0.016 | 1.000 |
| Te | 12.233 | 20.691 | 17.737 | 13.287 | 1.000 |
| $TeO_2$ | 5.105 | 0.000 | 4.966 | 0.000 | 1.000 |
| Ti | -26.013 | 2.574 | -44.141 | 3.984 | 1.000 |
| TiC | 2.217 | 16.605 | 2.743 | 20.441 | 1.000 |
| TiN | -5.802 | 7.471 | -9.902 | 12.338 | 1.000 |
| $TiO_2$ | 5.709 | 0.000 | 5.495 | 0.000 | 1.000 |
| TlBr | 5.803 | 0.000 | NaN | NaN | 1.000 |
| TlCl | 5.044 | 0.000 | NaN | NaN | 1.000 |
| V | -28.761 | 4.860 | -48.487 | 4.332 | 1.000 |
| VC | 2.780 | 15.372 | 3.003 | 18.509 | 1.000 |
| VN | -0.607 | 11.868 | -0.965 | 15.023 | 1.000 |
| W | -42.536 | 12.221 | -79.428 | 19.597 | 1.000 |
| $WS_2$ | 15.564 | 2.096 | 9.608 | 0.054 | 0.650 |
| $WSe_2$ | 27.018 | 5.273 | 16.265 | 1.574 | 0.650 |
| $Y_2O_3$ | 3.705 | 0.000 | 3.656 | 0.000 | 1.000 |
| $Y_3Al_5O1_2$ | 3.347 | 0.000 | 3.320 | 0.000 | 1.000 |
| $YLiF_4$ | 2.110 | 0.000 | 2.104 | 0.000 | 1.000 |
| $YVO_4$ | 3.987 | 0.000 | 3.910 | 0.000 | 1.000 |
| $Yb_2O_3$ | 3.772 | 0.000 | NaN | NaN | 1.000 |
| Zn | -31.413 | 13.506 | -46.256 | 23.846 | 1.000 |
| ZnO | 3.958 | 0.000 | 3.849 | 0.000 | 1.000 |
| ZnS | 5.524 | 0.000 | 5.361 | 0.000 | 1.000 |
| ZnSe | 6.517 | 0.292 | 6.127 | 0.221 | 1.000 |
| $ZnSiAs_2$ | 12.022 | 0.000 | NaN | NaN | 1.000 |
| ZnTe | 8.932 | 0.000 | 8.182 | 0.000 | 1.000 |
| Zr | -3.405 | 21.616 | 0.336 | 26.688 | 1.000 |
| $ZrO_2$ | 4.665 | 0.000 | NaN | NaN | 1.000 |

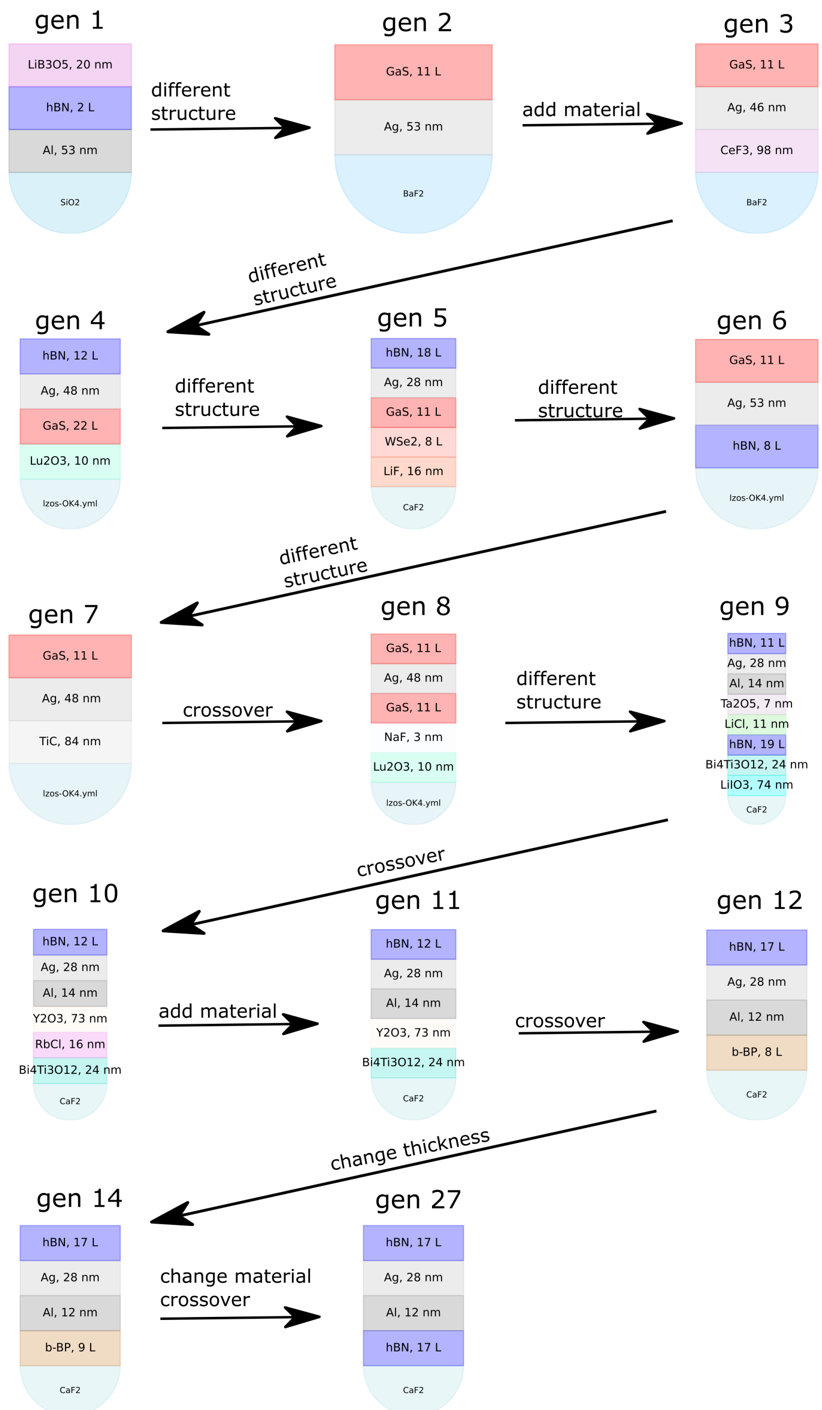


Figure S1: Scheme showing the evolution of the best-in-generation structures for the 633 nm single-mode sensor with respective mutations

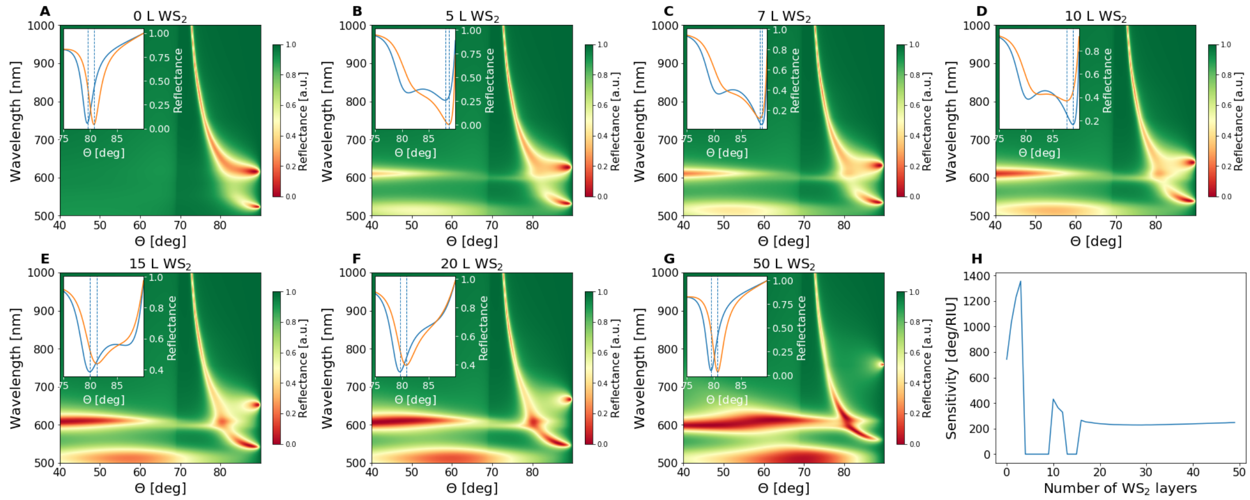


Figure S2: a-g) Dispersion curve of the dual-mode sensor with a reflectance spectrum of the sensor for n = 1.332 (blue curve) and n = 1.337 (orange curve) in inset for a structure with different number of $WS_2$ layers. h) Sensitivity of the SPR sensor as a function of number of $WS_2$ layers

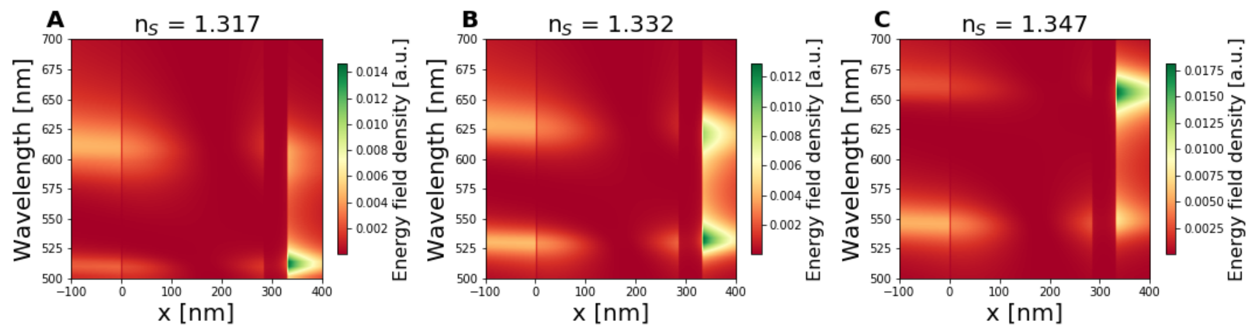


Figure S3: Energy field density of dual-mode SPR sensor with a) $n_S$=1.317, b) $n_S$=1.332, and c) $n_S$=1.347 shows energy redistribution between the modes

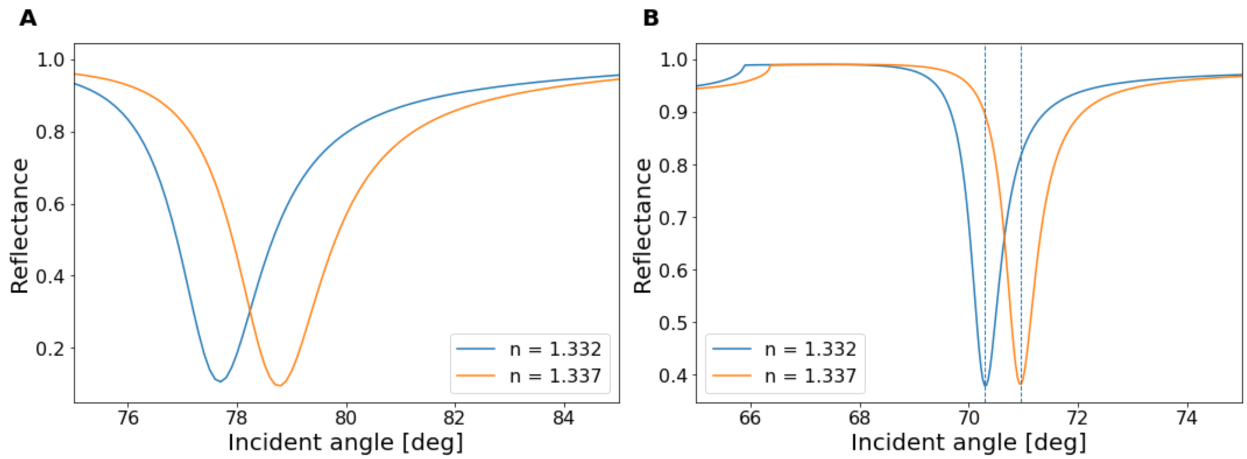


Figure S4: a) Reflectance spectrum of the sensor comprised of $CaF_2$ prism/47 nm Ag excited at a wavelength of 633 nm for $n_S = 1.332$ and $n_S = 1.337$ b) Reflectance spectrum of the sensor comprised of FSL3 prism/47 nm Ag excited at a wavelength of 785 nm for $n_S = 1.332$ and $n_S = 1.337$

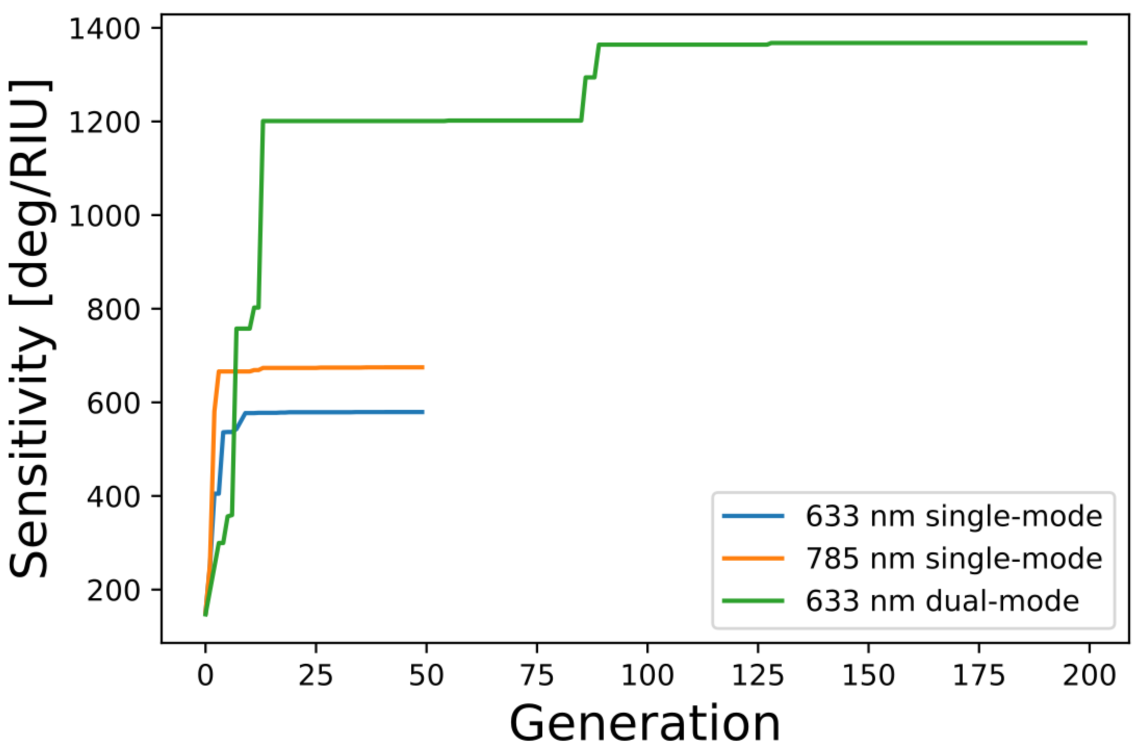


Figure S5: Evolution of the sensitivity of the best-generated sensors for single-mode sensor for 633 nm, single-mode sensor for 785 nm and dual-mode sensor for 633 nm.